applied sciences

MDPI

Article

Modification of 6,7-Dichloro-5,8-Quinolinedione at C2 Position: Synthesis, Quantum Chemical Properties, and Activity against DT-Diaphorase Enzyme

Monika Kadela-Tomanek *, Ewa Bębenek and Elwira Chrobak

Department of Organic Chemistry, Faculty of Pharmaceutical Sciences in Sosnowiec, Medical University of Silesia, Katowice, 4 Jagiellońska Str., 41-200 Sosnowiec, Poland
* Correspondence: mkadela@sum.edu.pl; Tel.: +48-32-3641666

Abstract: This research presents a synthesis and characterization of new 6,7-dichloro-5,8-quinolinedione derivatives with various groups at the C2 position. Chemical structures were examined by the spectroscopic methods. The quantum chemical parameters calculated using the DFT method showed that these derivatives are highly reactive towards the nucleophilic target. The molecular electrostatic potential map (MEP) showed that nucleophilic regions are localized near the nitrogen atom and the formyl group. Introduction of the hydroxyl or formyl groups at the C2 position led to the formation of an additional nucleophilic region. New compounds were tested as substrates for the NQO1 protein. An enzymatic study showed that derivatives are a good substrate for the NQO1 enzyme. Moreover, it was shown that the enzymatic conversion rates depend on the type of substituent at the C2 position of the 5,8-quinolinedione scaffold. A molecular docking study was used to study the interaction between new derivatives and the NQO1 protein. The arrangement and type of interactions between derivatives and the NQO1 enzyme depended on the type of substituent at the C2 position. A derivative with the hydroxyl group at this position was found to form an additional hydrogen bond between the formyl group and the tyrosine.

Keywords: 5,8-quinolinedione; DFT; NQO1; DT-diaphorase; molecular docking

Citation: Kadela-Tomanek, M.; Bębenek, E.; Chrobak, E. Modification of 6,7-Dichloro-5,8-Quinolinedione at C2 Position: Synthesis, Quantum Chemical Properties, and Activity against DT-Diaphorase Enzyme. *Appl. Sci.* **2023**, *13*, 1530. https://doi.org/10.3390/app13031530

Academic Editor: Tricia Naicker

Received: 26 December 2022
Revised: 17 January 2023
Accepted: 22 January 2023
Published: 24 January 2023

1. Introduction

DT-diaphorase (NQO1) is a flavoenzyme isolated by Ernster and coworkers over 60 years ago [1,2]. The enzyme is localized mainly in cytosol, but its low level is also detected in the nucleus. In normal human tissues, a high level of this protein is observed in many epithelial cells and in the vascular endothelium and adipocytes. The NQO1 enzyme is highly expressed in most human solid tumors, such as lung, breast, colon, and pancreas. Moreover, an increase in protein expression is detected in preneoplastic lesion and liver cancer [2–7]. The crystal structure of human NQO1 was described in 2000 [8]. Human NQO1 is a dimer consisting of two identical subunits, between which there are two active sites composed of residues of polypeptide chains. Each dimer is bound to the flavin adenine dinucleotide (FAD) [3,9]. The molecular mechanism is based on the direct two-electron-mediated reduction of quinone to a hydroquinone scaffold [10,11]. The role of NQO1 in cancer treatment has been repeatedly analyzed and described in the literature [2,4,12,13]. Dicoumarol is a well-known inhibitor of NQO1, which causes an oxidative stress in the cell (Figure 1). It generates numerous side effects, such as disorders of the blood clotting cycle by inhibiting the vitamin K oxidoreductase [14–16]. In contrast, streptonigrin (ST) is a substrate for NQO1. By-products of the reaction between streptonigrin (ST) and NQO1 are the reactive oxygen species (ROS) that cause the mutation of DNA (Figure 1). The high toxicity of streptonigrin (ST) prevents its use in cancer treatment [17–20].

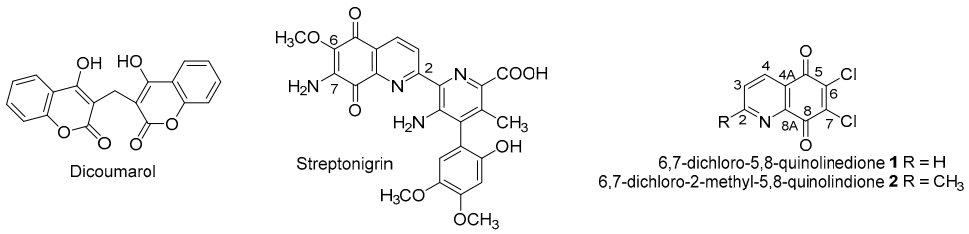

Figure 1. The chemical structure of a quinone compound.

The study of the structure–activity relationship showed that a key fragment necessary to preserve the bioactivity of streptonigrin (ST) is the 5,8-quinolinedione moiety. Further research has shown that the bioactivity depends on the substituents at the C2, C6, and C7 positions of the 5,8-quinolinedione moiety [19]. The introduction of an amine or alkoxyl group at the C6 or/and C7 positions increases the cytotoxicity against leukemia, melanoma, breast, cervix, ovary, and lung cancers [21–26]. The halogen atom at the C6 and/or C7 positions also influences the antitumor activity. Yoo et al. showed that compounds with chloride atom exhibited higher activity than those with bromide atom [27]. Comparing the activity and biochemical properties of different derivatives of streptonigrin showed that a substituent at the C2 position influences their interaction with metal ions [19].

Many synthetic 5,8-quinolinedione compounds exhibiting biological activity have been described in the literature [21]. Studies on the modification of 5,8-quinolinedione at the C2 position are rarely found in the literature. The introduction of a methyl group at this position, such as 6,7-dichloro-2-methyl-5,8-quinolinedione **2**, significantly affects the biological activity compared with 6,7-dichloro-5,8-quinolinedione **1**. Moreover, derivative **2** was characterized by lower toxicity against a normal cell line than compound **1** [24,28].

In this work, we present the synthesis of new derivatives of 6,7-dichloro-5,8-quinolonedione, which contain formyl, hydroxyl groups, or chlorine atom as a substituent at the C2 position. These derivatives were characterized by the quantum chemical parameters calculated by the DFT method. The in silico bioavailability of compounds was determined using the pkCSM program. They were also tested as substrates for the NQO1 enzyme. The molecular docking study was used to examine the interaction between derivatives and the NQO1 enzyme.

2. Materials and Methods

2.1. Physical Measurements

Nuclear magnetic resonance (NMR) spectra were recorded with a Bruker Avance 600 spectrometer (Bruker, Billerica, MA, USA) in $CDCl_3$ solvent. High-resolution mass spectral analysis (HRMS) was performed using a Bruker Impact II instrument (Bruker, Billerica, MA, USA). The sample was dissolved in a mixture of acetonitrile and 1% formic acid in a ratio of 4:1.

2.2. Chemistry

All reagents were purchased from Merck (Darmstadt, Germany), and their purity was higher than 98%. 6,7-Dichloro-2-methyl-5,8-quinolinedione **2**, 2-hydroxyquinoline-8-ol **4**, and 2-chloroquinoline-8-ol **5** were synthesized according to the literature methods [28,29].

2.2.1. Synthesis of 6,7-Dichloro-5,8-Dioxo-5,8-Dihydroquinoline-2-Carbaldehyde 3

Selenium dioxide (1.15 g; 0.01 mol) was dissolved in 70 mL dioxane and 1 mL water and warmed to 60 °C. In this temperature, a mixture of 6,7-dichloro-2-methyl-5,8-quinolinedione (0.605 g; 0.0025 mol) in 15 mL dioxane was added. The mixture was stirred at reflux for 6 h. After then, the reaction mixture was concentrated with a vacuum evaporator. The crude product was purified by a column chromatography method to give pure product **3** (0.416 g; 0.0016 mol; yield 65%; purity 99.8%). Mp. 202–203 °C. ^{1}H NMR ($CDCl_3$, 600 MHz) δ 8.40, 8.53, 10.35; ^{13}C NMR ($CDCl_3$, 150 MHz) δ 125.2, 130.4, 137.5, 143.6,

145.1, 147.0, 155.9; 173.7, 175.0, 191.4; HRAPCIMS *m*/*z* 255.9571 (calcd for $C_{10}H_4Cl_2NO_3$, 255.9568) (Figure S1).

2.2.2. Synthesis of 2-Substituted-5,8-Quinolinedione 6–7

The 2-substitutedquinoline-8-ol **4–5** (0.003 mol) was dissolved in 6 mL hydrogenic acid and was heated to 60 °C. In this temperature, the water solution of sodium chlorate (0.386 g in 1.7 mL water) was added. After 1 h, the mixture was dissolved in 43 mL water. The resulting participate was filtered under reduce pressure. The product was purified by a column chromatography method to give:

6,7-dichloro-2-hydroxy-5,8-quinolinedione **6** (0.322 g; 0.0013 mol; yield 44%; purity 99.6%). Mp. 209–210 °C. ^{1}H NMR ($CDCl_3$, 600 MHz) δ 6.85, 7.94, 8.10; ^{13}C NMR ($CDCl_3$, 150 MHz) δ 128.0, 133.0, 135.7, 137.1, 143.7, 144.9, 156.4; 171.3, 172.9; HRAPCIMS *m*/*z* 243.9561 (calcd for $C_9H_4Cl_2NO_3$, 243.9568) (Figure S2).

2,6,7-Trichloro-5,8-chinolinodion **7** (0.402 g; 0.0015 mol; yield 51%; purity 99.4%). Mp. 216–217 °C. ^{1}H NMR ($CDCl_3$, 600 MHz) δ 7.55, 8.47; ^{13}C NMR ($CDCl_3$, 150 MHz) δ 123.9, 128.7, 136.6, 138.1, 144.2, 146.8, 151.1; 174.9, 176.8; HRAPCIMS *m*/*z* 261.9926 (calcd for $C_9H_3Cl_3NO_2$, 21.9929) (Figure S3).

2.3. Computational Details

The optimized chemical structures of compounds **3** and **6–7** were calculated using the DFT (B3LYP/6-311G+(d,p)) method implemented in the Gaussian 09 program package [30]. The obtained optimized structures are presented in Figure S4.

The optimized structure of compound **3** was used to calculate the ^{1}H and ^{13}C NMR spectra. The NMR spectra were calculated using the gauge-independent atomic orbital (GIAO) method implemented in the Gaussian 09 program package [30–32]. The calculated geometry was used to determine the HOMO-LUMO energy, quantum chemical descriptors, molecular electrostatic potential, and molecular docking study [33]. All obtained results were visualized in the GaussView Version 5 software package [34].

The ADMET parameters were determined using the pkCSM software [35,36].

2.4. Enzymatic Assay

Compounds **1–3** and **6–7** were tested as NQO1 substrates using the NADPH recycling assay according to the literature method [37,38]. The recombinant NQO1 (DT-diaphorase, EC 1.6.5.5, human recombinant, Sigma-Aldrich) was used, and the oxidation of NADPH to $NADP^+$ was measured at an absorption wavelength of 340 nm on a BioTek 800TS microplate reader (Biokom, Poland). Compounds were dissolved in dimethyl sulfoxide (2 µL) and added to a 96-well plate. The NQO1 protein (1.4 µg/mL) in 50 mmol/L potassium phosphate buffer (pH = 7.4) was added to each well (198 µL) (Nunc, Thermo Fisher Scientific, Waltham, MA, USA). Once the 96-well plate was filled with the assay solutions, except the NADPH solution, it was placed into the instrument and left to sit for 5 min before starting the measurements. The enzymatic reaction was initiated by automatically dispensing the NADPH solution into the wells, and data were recorded at 10 s intervals for 5 min at 25 °C. The linear part of the absorbance vs. time graphs (the first 20 s to 1 min) was fitted, and the slops were calculated. NADPH oxidation rates were compared with reactions lacking a tested compound. Initial velocities were calculated, and data expressed as µmol NADPH/µmol NQO1/min. All reactions were carried out at least in triplicate.

2.5. Molecular Docking Study

A molecular docking study was performed using the crystal structure of the human NQO1 protein, which was collected from the Protein Data Bank (PDB) database with the PDB identifier 2F1O [39]. During docking, the FAD molecules were presented into binding sites as cofactors.

A molecular docking study was performed with the AutoDock Vina 1.5.6. software package [40]. The grid center of Vina docking was selected as the center of reference ligands, which accompanied the downloaded protein complexes. For NQO1, its search grid was recognized to be center_x: 11.456, center_y: 12.048, and center_z: −5.677, and the dimensions were size_x: 15, size_y: 15, and size_z: 15. Default values of all other parameters were used, and the complexes were submitted to 8 genetic algorithm runs. All obtained results were visualized using the BIOVIA Discovery Studio Visualizer v17.2.0.16349 software package [41].

3. Results and Discussion

3.1. Chemistry

Oxidation of 6,7-dichloro-2-methyl-5,8-quinolinedione **2** with selenium dioxide in the presence of dioxane gave 6,7-dichloro-5,8-dioxo-5,8-dihydroquinoline-2-carbaldehyde **3** (Scheme 1).

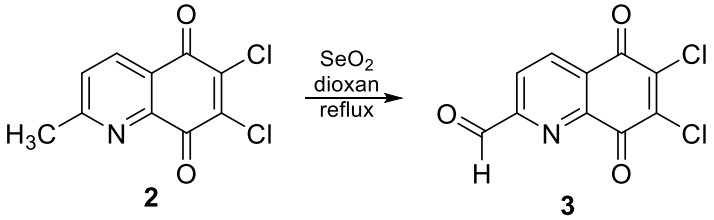

Scheme 1. Synthesis of 6,7-dichloro-5,8-dioxo-5,8-dihydroquinoline-2-carbaldehyde **3**.

2-Hydroxy-5,8-quinolinedione **6** and 2-chloro-5,8-quinolinedione **7** were obtained by oxidation of 2-hydroxyqinolin-8-ol **4** or 2-chloroquinolin-8-ol **5**, respectively, in the presence of sodium chlorate and hydrochloric acid at 60 °C (Scheme 2).

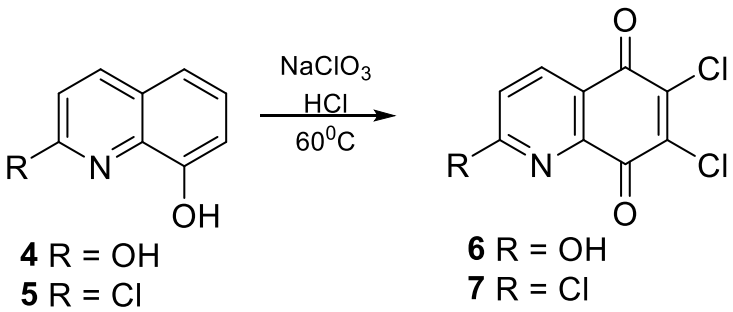

Scheme 2. Synthesis of 6,7-dichloro-2-hydroxy-5,8-quinolinedione **6** and 2,6,7-trichloro-5,8-chinolinodion **7**.

Chemical structures of derivatives **3**, **6–7** were characterized by the ^{1}H and ^{13}C NMR spectroscopic methods. Moreover, for compound **3**, the 2D (HSQC and HMBC) NMR spectra were performed.

Three signals were observed in the ^{1}H NMR spectrum of compound **3** (Table 1). The chemical shift of the proton at the formyl group was observed at 10.35 ppm. Signals located at 8.77 and 8.40 ppm were assigned to the protons at the H4 and H3 positions, respectively. The signals at 191.4, 137.5, and 125.2 ppm were assigned to the carbon atoms at the formyl group and at the C4 and C3 positions, respectively (Table 1 and Figure S5).

Table 1. The chemical shifts (^{1}H NMR and ^{13}C NMR spectra) and correlations proton–carbon (HSQC and HMBC experiments) for derivative **3**.

Proton	^{1}H NMR δ (ppm)	HSQC	Carbon	^{13}C NMR δ (ppm)	HMBC
CHO	10.35	10.35–191.4	CHO	191.4	10.35–155.9 (C2) 10.35–125.2 (C3) 10.35–137.5 (C4)
H4	8.77	8.77–137.5	C4	137.5	8.77–147.0 (C8A) 8.77–155.9 (C2) 8.77–175.0 (C5)
H3	8.40	8.40–125.6	C3	125.2	8.40–130.4 (C4A) 8.40–155.8 (C2) 8.40–191.4 (CHO)

The HMBC spectrum shows that the proton at the formyl group correlates with the carbon atoms at the C2 (155.9 ppm), C3 (125.2 ppm), and C4 (137.5 ppm) positions. The spectrum shows also a correlation of proton at the H4 position with the carbon atoms at the C5 (175.0 ppm), C2 (155.9 ppm), and C8A (147.0 ppm) positions. Another correlation was observed between the proton at the H3 position and carbon atoms at the C2 (155.9 ppm) and C4A (130.4 ppm) positions (Table 1 and Figure S6).

In the HMBC spectrum, a correlation between carbon atoms at the C6, C7, and C8 positions was not observed. For this reason, a simulation of the NMR spectrum was performed using the GIAO method [42,43]. The experimental and calculated chemical shifts for compound **3** are presented in Table 2.

Table 2. The experimental and calculated ^{1}H NMR and ^{13}C NMR spectra of derivative **3**.

Atoms	Chemical Shift δ (ppm)	
	Experimental	Calculated
CHO	10.35	11.63
H4	8.77	8.69
H3	8.40	7.73
CHO	191.4	194.8
C2	155.9	166.1
C3	125.2	124.9
C4	137.5	134.1
C4A	130.4	126.5
C5	175.0	177.5
C6	143.6	152.8
C7	145.1	154.2
C8	173.7	174.8
C8A	147.0	152.9

According to the calculated spectrum, the signal at 173.7 ppm was assigned to the carbon atom at the C8 position. The chemical shifts of carbon atoms at the C6 and C7 positions were observed at 143.6 and 145.1 ppm, respectively. Figure 2 shows a good agreement between experimental and calculated ^{13}C and ^{1}H NMR spectra for compound **3** (R = 0.9756 and R = 0.9991, respectively).

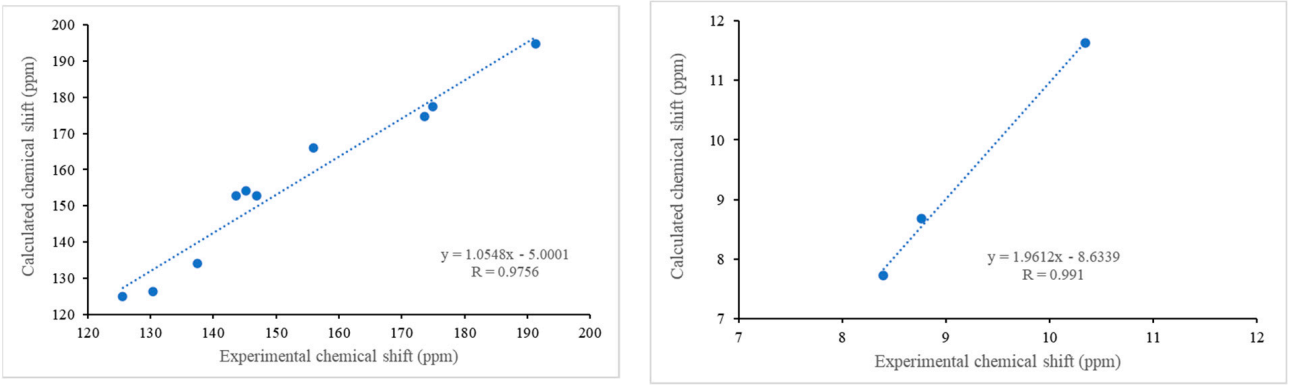

Figure 2. The linear regression between the experimental and calculated (**a**) ^{13}C NMR; (**b**) ^{1}H NMR chemical shift of compound **3**.

3.2. Quantum Chemical Properties

The quantum chemical parameters depend on the localization and energy of the highest occupied molecular orbital (HOMO) and lowest unoccupied molecular orbital (LUMO). The energy gap influences the ionization potential (I), electron affinity (A), hardness (η), chemical potential (μ), electronegativity (χ), and electrophilicity index (ω) [44,45].

As seen in Figure 3, the delocalization of the HOMO orbital depends on the type of a substituent at the C2 position of the 5,8-quinolinedione scaffold. The HOMO orbital for compound **3** is localized close to the formyl group at the C2 position, while for derivatives **6–7**, it is delocalized at the 5,8-quinolinedione scaffold (Figure 3). The LUMO orbitals for all compounds are delocalized at the 5,8-quinolinedione scaffold. The arrangement of orbitals across the entire molecule indicates that the molecular system has good charge transfer capabilities (Figure 3).

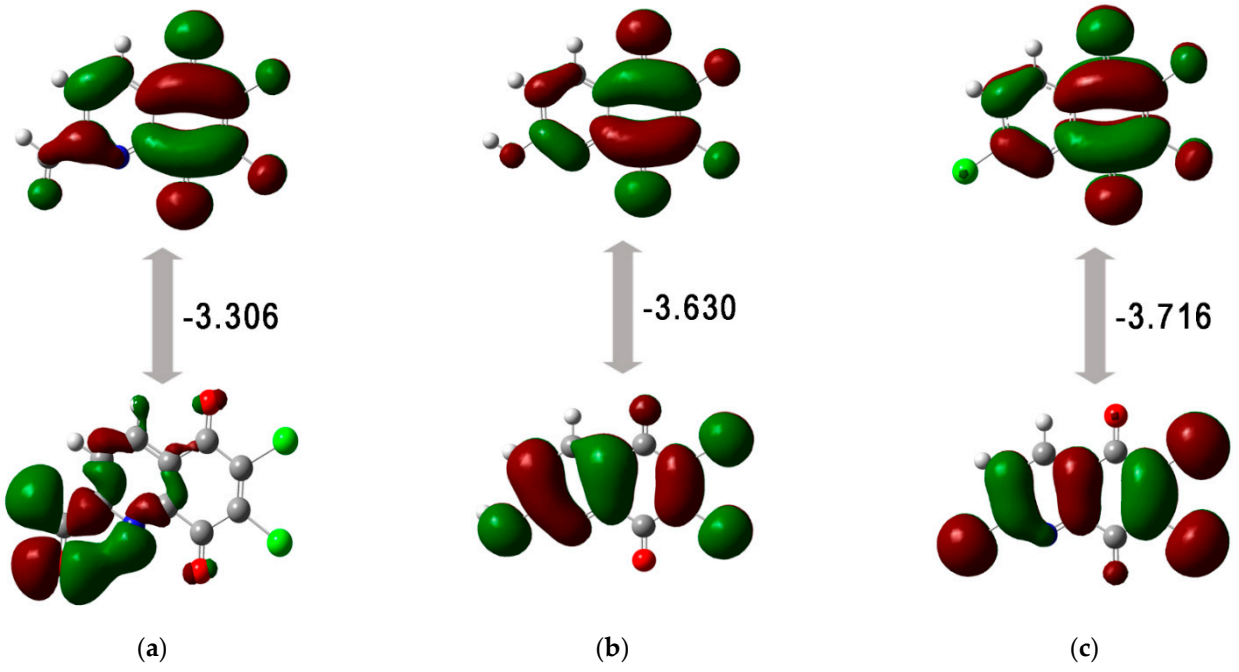

Figure 3. The arrangement of orbitals for compounds: (**a**) **3**, (**b**) **6**, (**c**) **7**.

The tested compounds show the energy gap (ΔE) ranging from −3.306 to −3.716 eV, which means that they can exhibit high reactivity towards the biological target [46]. The type of substituent at the C2 position of 5,8-quinolinedione slightly influences the energy gap (ΔE). The quantum chemical descriptors are presented in Table 3.

Table 3. The quantum chemical descriptors for compounds **3** and **6–7**.

Compound	E_{HOMO}	E_{LUMO}	ΔE	I	A	η	μ	χ	ω
3	−7.865	−4.559	−3.306	7.865	4.559	1.653	−6.212	6.212	11.672
6	−7.860	−4.230	−3.630	7.860	4.230	1.815	−6.045	6.045	10.066
7	−8.281	−4.564	−3.716	8.281	4.564	1.858	−6.422	6.422	11.100

The quantum chemical descriptors show that compounds **3** and **6–7** are characterized by high softness and flexibility in gaining electrons. The high values of the electronegativity (χ) and electrophilicity index (ω) indicate that these molecules are good acceptors for the nucleophilic target.

The distribution of the electrophilic and nucleophilic regions in the molecule is described by the MEP map [47,48]. Different colors on the MEP map represent the different charges. The red, blue, and green regions are negative, positive, or neutral, respectively, [49]. As seen in Figure 4, the negative areas are localized near the oxygen and nitrogen atoms. The positively charged region is localized near the hydrogen atom at the 5,8-quinolinedione moiety, and the neutral regions are visible near the chlorine atoms.

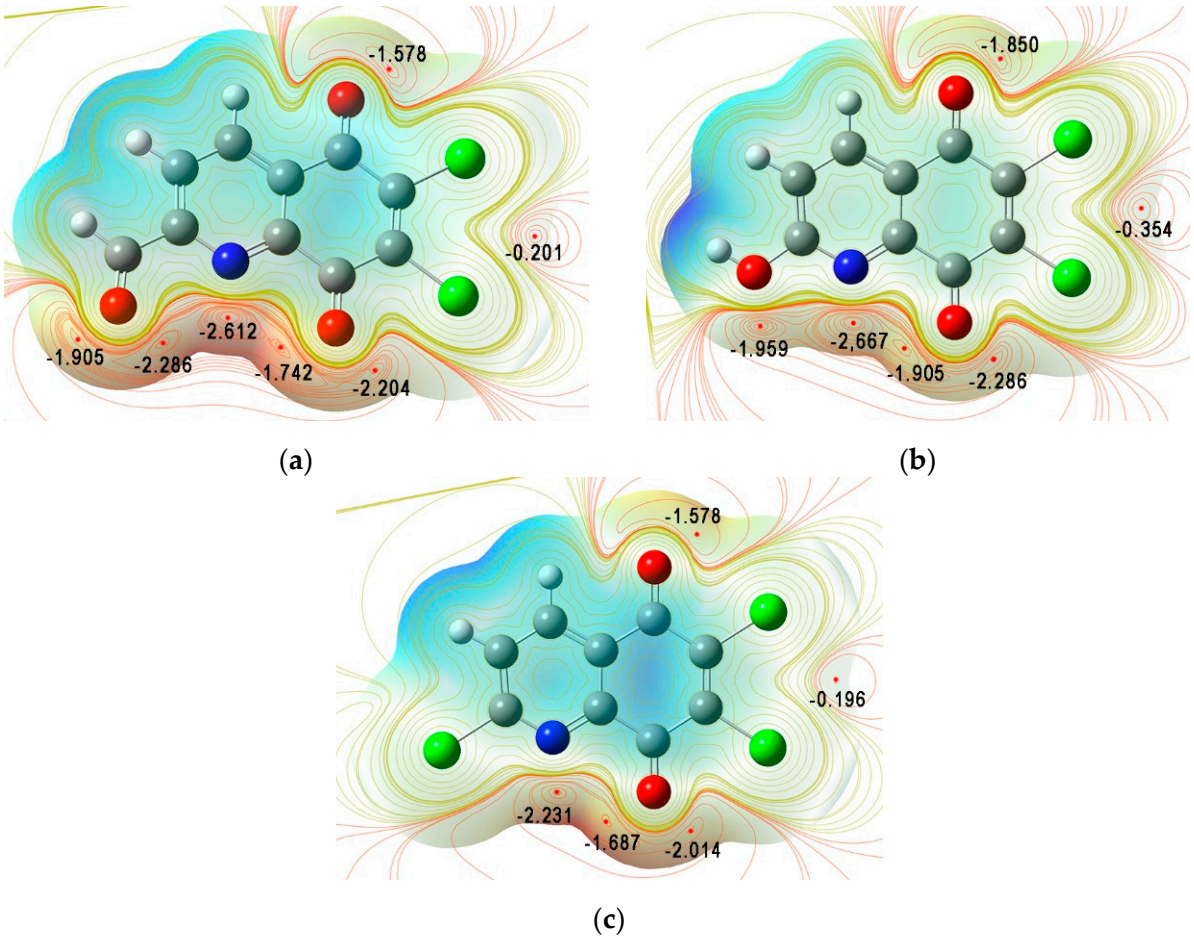

Figure 4. The MEP map for compounds: (**a**) **3**, (**b**) **6**, (**c**) **7**.

For all compounds, the three main areas of negative electrostatic potential are observed. The first area includes the substituent at the C2 position, nitrogen atom, and formyl group at the C8 position. In this area, the type of substituent significantly influences an electrostatic potential. According to the literature [28], for 6,7-dichloro-2-methylo-5,8-quinolinedione **2**, three potential minima near the nitrogen atom and oxygen of the formyl group at the C8 position were observed. Replacing the methyl group by the chlorine atom does not affect the arrangement of the electrostatic potential. The introduction of a substituent with an oxygen atom, such as hydroxyl (**6**) and formyl (**3**) groups, led to an additional local potential minimum near the substituent at the C2 position. For molecule **3**, two local potential minima are observed, both near the formyl group at the C2 position, and they are equal to −1.905 and −2.286 eV, respectively. For compound **6**, the potential minimum is located near the hydroxyl group reaching a value of −1.959 eV. The second and third areas for all molecules include the formyl group at the C5 position and chlorine atoms at the C6 and C7 positions, respectively. The electrostatic potentials in these two areas do not depend on the type of group at the C2 position.

3.3. ADMET Analysis

The in silico analysis including absorption, distribution, metabolism, excretion, and toxicity (ADMET) is a useful tool to predict the bioavailability of the tested compound [50,51]. The ADMET parameters such as solubility (logS), lipophilicity (logP), molecular mass (MW), and number of acceptors (HA) and donors (HD) of the hydrogen bond for compounds **1–3** and **6–7** were determined using the pkCSM software [35]. The toxicity was predicted by the lethal concentration values (LC_{50}) and hepatotoxicity (Table 4).

Table 4. The ADMET parameters for compounds **1–3** and **6–7** [35].

Compound	logS	logP	MW (g/mol)	HA	HD	LC_{50} (mM)	Hepatotoxicity
1	−3.08	2.14	228	3	0	8.710	No
2	−3.39	2.45	242	3	0	6.531	No
3	−3.01	1.96	256	4	0	8.810	No
6	−3.04	1.86	244	4	1	28.249	No
7	−3.87	2.80	262	3	0	8.790	No

According to the ESOL solubility class [52], a logS value between −4 and −2 means that the substance is soluble in water. The tested compounds **1–3** and **6–7** show good solubility in water. The introduction of a methyl group or chlorine atom at the C2 position decreases the solubility. Compounds with the formyl (**3**) and hydroxyl (**6**) groups have a solubility comparable to that of 6,7-dichloro-5,8-quinolinedione **1**.

All compounds (**1–3** and **6–7**) are characterized by a good oral availability according to the Lipinski rules, which means that they have low lipophilicity (logP < 5) and molecular mass (MW < 500). Moreover, the number of acceptors (HA) and donors (HD) of the hydrogen bond are below 10 and 5, respectively.

The lethal concentration value (LC_{50}) is a concentration of a compound causing the death of 50% of *fathead minnows*. If the LC_{50} is less than 0.5 mM, the compound has high acute toxicity [35,36]. The in silico analysis shows that the LC_{50} for tested compounds (**1–3** and **6–7**) is in the range of 6.531 mM to 28.249 mM, which mean that they have low toxicity. It can be assumed that these derivatives do not interfere with liver function (Table 4).

3.4. Enzymatic Study

Compounds **1–3**, **6–7**, and streptonigrin (ST) were tested as a substrate for the NQO1 according to the literature methods [13,22,23]. Results are presented in Figure 5.

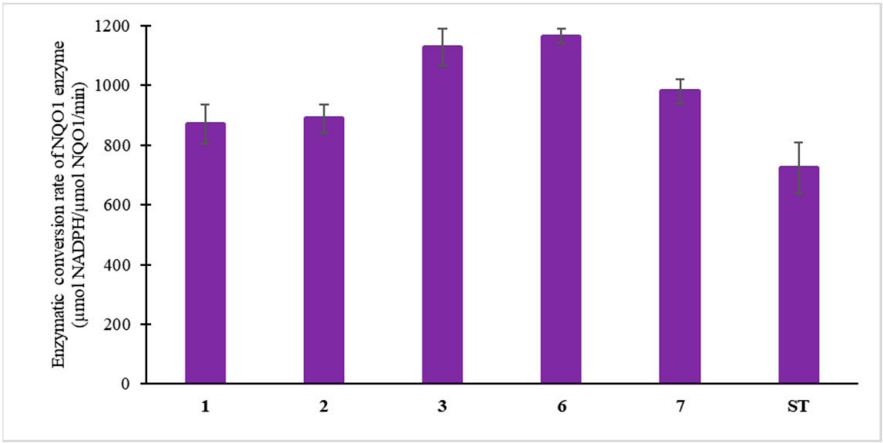

Figure 5. Enzymatic conversion rate of NQO1 of compounds **1–3**, **6–7**, and streptonigrin (ST).

The derivatives **1–3** and **6–7** show a higher enzymatic conversion rate of the NQO1 protein than reference substance (**ST**), indicating that they are good substrates for NQO1. 6,7-Dichloro-5,8-quinolinedione **1** and 6,7-dichloro-2-methylo-5,8-quinolinedione **2** exhibit comparable conversion rates, which are equal to 872 µmol NADPH/µmol NQO1/min and 890 µmol NADPH/µmol NQO1/min, respectively. The oxidation of methyl to the formyl group (compound **3**) increases the conversion rate. A similar effect is observed for compounds with a hydroxyl group (derivatives **6**) and chloride atom (derivatives **7**) at the C2 position. These results show that the introduction of various groups at the C2 position increases the enzymatic conversion rate of the NQO1 enzyme, and it depends on the type of substituent.

3.5. Molecular Docking Study

A molecular docking study was used to check the interaction between the NQO1 enzyme and compounds **1–3**, **6–7**, and streptonigrin (ST). The structure of the enzyme as a complex with the flavin adenine dinucleotide (FAD) cofactor was downloaded from the PDB (PDB ID:2F1O). The scoring values (ΔG) of all molecules are presented in Table 5. The lowest value of ΔG corresponds to a strong binding affinity and the most probable ligand–protein complexes in vitro.

Table 5. Scoring values (ΔG) of molecules **1–3**, **6–7**, and **ST**.

Molecules	ΔG (kcal/mol)
1	−8.1
2	−8.0
3	−8.3
6	−8.3
7	−8.2
ST	−7.1

The scores of protein–ligand complexes range from −8.0 to −8.3 kcal/mol. All dichloro-5,8-quinolindiones (**1–3** and **5–6**) have lower scores than streptonigrin (ST), indicating their strong binding affinity.

Complete models of interaction between the NQO1 enzyme and ligands **1–3** and **6–7** are presented in Figure 6. Details on the type and length of the bonds are summarized in Table S1.

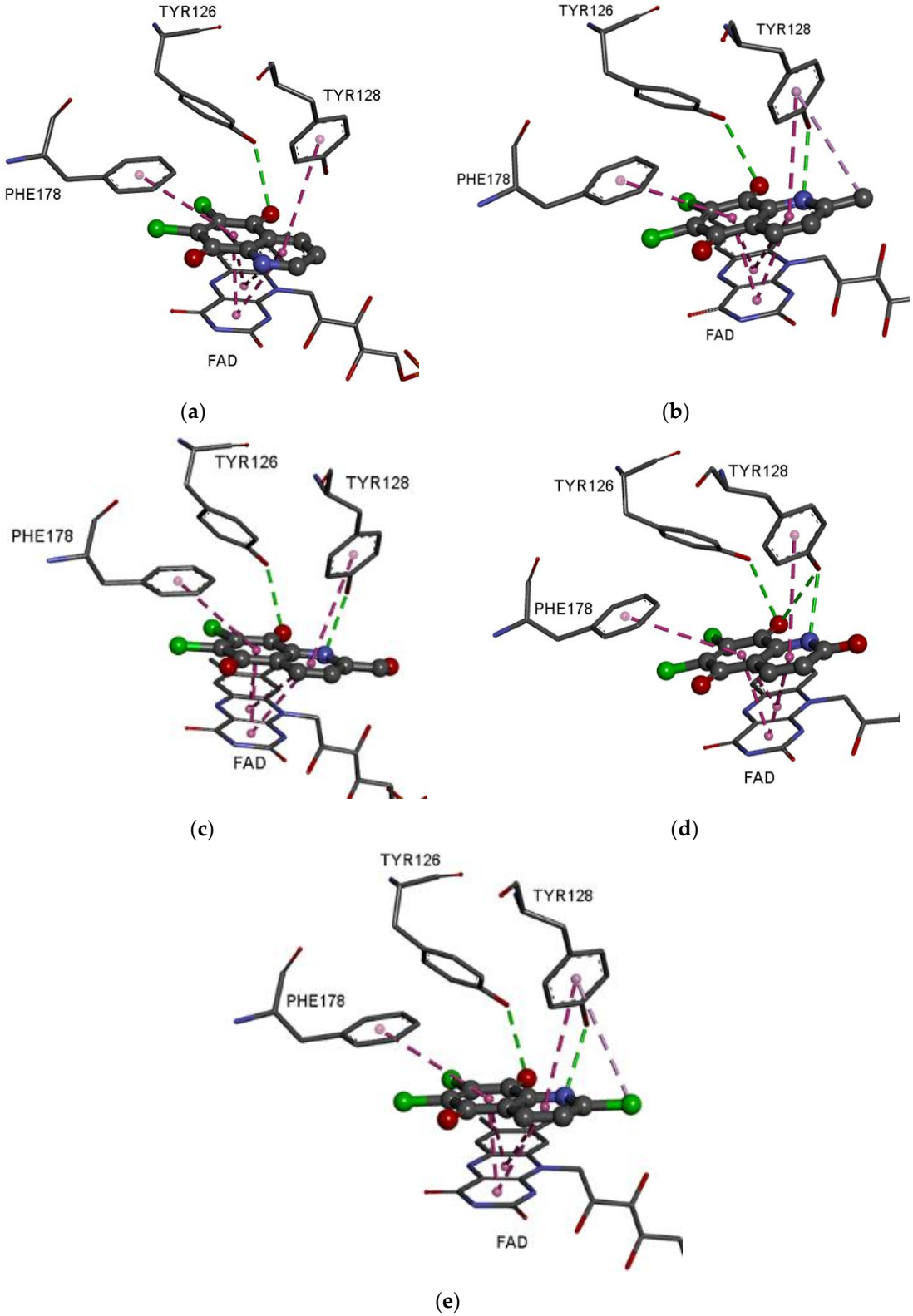

Figure 6. Visualization of interactions between the NQO1 enzyme and derivatives: (**a**) **1**, (**b**) **2**, (**c**) **3**, (**d**) **6**, (**e**) **7**.

6,7-Dichloro-5,8-quinolinedione **1** creates the hydrogen bond between the formyl group at the C8 position and tyrosine (TYR126) as well as hydrophobic interactions with phenylalanine (PHE178), tyrosine (TYR128), and the FAD cofactor. Molecules with a substituent at the C2 position (**2–3** and **6–7**) create also the hydrogen bond between nitrogen

atom and tyrosine (TYR126). Additionally, in the complex of 6,7-dichloro-2-hydroxy-5,8-quinolinedione **6** with NQO1, a hydrogen bond is observed between the formyl group at the C8 position and tyrosine (TYR126).

4. Conclusions

Research has shown that the new derivatives of 6,7-dichloro-5,8-quinolinedione are characterized by a number of properties that can be important for their biological activity. The quantum chemical properties showed that they are highly reactive towards the nucleophilic target. The in silico ADMET analysis showed that compounds are characterized by a good oral availability and low toxicity against *fathead minnows*. The enzymatic study showed that they are a good substrate for the NQO1 enzyme. Moreover, it was also found that the enzymatic conversion rates depend on the type of substituent at the C2 position of the 5,8-quinolinedione scaffold. A compound with the substituted hydroxyl group at this position exhibited the highest activity. A molecular docking study revealed that the arrangement and type of interactions between the derivatives and the NQO1 enzyme depend on the type of substituent at the C2 position. In the case of a compound with the substituted hydroxyl group, an additional hydrogen bond between the formyl group and tyrosine was observed.

Supplementary Materials: The following supporting information can be downloaded at: https://www.mdpi.com/article/10.3390/app13031530/s1, Figure S1: Spectra of 6,7-dichloro-5,8-dioxo-5,8-dihydroquinoline-2-carbaldehyde **3**; Figure S2: Spectra of 6,7-dichloro-2-hydroxy-5,8-quinolinedione **6**; Figure S3: Spectra of 2,6,7-trichloro-5,8-chinolinodion **7**; Figure S4: The optimized structure of 5,8-quinolinedione compounds **3** and **6–7**; Figure S5: The ^{1}H-^{13}C HSQC spectrum (600 MHz, $CDCl_3$) of compound **3**; Figure S6: The ^{1}H-^{13}C HMBC spectrum (600 MHz, $CDCl_3$) of compound **3**; Table S1: Interaction of compounds **1–3** and **6–7** with an active site of the NQO1 protein.

Author Contributions: Conceptualization, methodology, writing—original draft preparation, M.K.-T.; methodology, E.C. and E.B. All authors have read and agreed to the published version of the manuscript.

Funding: This research was funded by the Medical University of Silesia in Katowice, Poland. Grant PCN-2-027/K/2/F.

Institutional Review Board Statement: Not applicable.

Informed Consent Statement: Not applicable.

Data Availability Statement: Not applicable.

Conflicts of Interest: The authors declare no conflict of interest.

References

1. Ernster, L. Diaphorase activities in liver ctoplasmic fractions. *Fed. Proc.* **1958**, *17*, 216.
2. Ross, D.; Siegel, D. The diverse functionality of NQO1 and its roles in redox control. *Redox Biol.* **2021**, *41*, 101950. [CrossRef]
3. Beaver, S.K.; Mesa-Torres, N.; Pey, A.L.; Timson, D.J. NQO1: A target for the treatment of cancer and neurological diseases, and a model to understand loss of function disease mechanisms. *Biochim. Biophys. Acta Proteins Proteom.* **2019**, *1867*, 663–676. [CrossRef] [PubMed]
4. Siegel, D.; Ross, D. Immunodetection of NAD(P)H:quinone oxidoreductase 1 (NQO1) in human tissues. *Free Radic. Biol. Med.* **2000**, *29*, 246–253. [CrossRef] [PubMed]
5. Siegel, D.; Franklin, W.A.; Ross, D. Immunohistochemical detection of NAD(P)H:quinone oxidoreductase in human lung and lung tumors. *Clin. Cancer Res.* **1998**, *4*, 2065–2070.
6. Strassburg, A.; Strassburg, C.P.; Manns, M.P.; Tukey, R.H. Differential gene expression of NAD(P)H:quinone oxidoreductase and NRH:quinone oxidoreductase in human hepatocellular and biliary tissue. *Mol. Pharmacol.* **2002**, *61*, 320–325. [CrossRef]
7. Schor, N.A.; Morris, H. The activity of the DT-diaphorase in experimental hepatomas. *Cancer Biochem. Biophys.* **1977**, *2*, 5–9.
8. Faig, M.; Bianchet, M.; Winski, S.; Hargreaves, R.; Moody, C.; Hudnott, A.; Ross, D.; Amzel, L. Structure-based development of anticancer drugs: Complexes of NAD(P)H:quinone oxidoreductase 1 with chemotherapeutic quinones. *Structure* **2001**, *9*, 659–667. [CrossRef] [PubMed]
9. Li, R.; Bianchet, M.A.; Talalay, P.; Amzel, L.M. The three-dimensional structure of NAD(P)H:quinone reductase, a flavoprotein involved in cancer chemoprotection and chemotherapy: Mechanism of the two-electron reduction. *Proc. Natl. Acad. Sci. USA* **1995**, *92*, 8846–8850. [CrossRef]

10. Iyanagi, T.; Yamazaki, I. One-electron-transfer reactions in biochemical systems. V. Difference in the mechanism of quinone reduction by the NADH dehydrogenase and the NAD(P)H dehydrogenase (DT-diaphorase). *Biochim. Biophys. Acta* **1970**, *216*, 282–294. [CrossRef]
11. Tedeschi, G.; Chen, S.; Massey, V. DT-diaphorase. Redox potential, steady-state, and rapid reaction studies. *J. Biol. Chem.* **1995**, *270*, 1198–1204. [CrossRef] [PubMed]
12. Belinsky, M.; Jaiswal, A.K. NAD(P)H:quinone oxidoreductase1 (DT-diaphorase) expression in normal and tumor tissues. *Cancer Metastasis Rev.* **1993**, *12*, 103–117. [CrossRef]
13. Wu, L.Q.; Ma, X.; Zhang, C.; Liu, Z.P. Design, synthesis, and biological evaluation of 4-substituted-3,4-dihydrobenzo[h]quinoline-2,5,6(1H)-triones as NQO1-directed antitumor agents. *Eur. J. Med. Chem.* **2020**, *198*, 112396. [CrossRef] [PubMed]
14. Timson, D.J. Dicoumarol: A drug which hits at least two very different targets in vitamin K metabolism. *Curr. Drug Targets* **2017**, *18*, 500–510. [CrossRef] [PubMed]
15. Cullen, J.J.; Hinkhouse, M.M.; Grady, M.; Gaut, A.W.; Liu, J.; Zhang, Y.P.; Weydert, C.J.; Domann, F.E.; Oberley, L.W. Dicumarol inhibition of NADPH:quinone oxidoreductase induces growth inhibition of pancreatic cancer via a superoxide-mediated mechanism. *Cancer Res.* **2003**, *63*, 5513–5520. [PubMed]
16. Lewis, A.; Ough, M.; Li, L.; Hinkhouse, M.M.; Ritchie, J.M.; Spitz, D.R.; Cullen, J.J. Treatment of pancreatic cancer cells with dicumarol induces cytotoxicity and oxidative stress. *Clin. Cancer Res.* **2004**, *10*, 4550–4558. [CrossRef] [PubMed]
17. Siegel, D.; Yan, C.; Ross, D. NAD(P)H:quinone oxidoreductase 1 (NQO1) in the sensitivity and resistance to antitumor quinones. *Biochem. Pharmacol.* **2012**, *83*, 1033–1040. [CrossRef]
18. Bolzán, A.D.; Bianchi, M.S. Genotoxicity of streptonigrin: A review. *Mutat. Res.* **2001**, *488*, 25–37. [CrossRef]
19. Bringmann, G.; Reichert, Y.; Kane, V. The total synthesis of streptonigrin and related antitumor antibiotic natural products. *Tetrahedron* **2004**, *30*, 3539–3574. [CrossRef]
20. Donohoe, T.J.; Jones, C.R.; Kornahrens, A.F.; Barbosa, L.C.A.; Walport, L.J.; Tatton, M.R.; O'Hagan, M.; Rathi, A.H.; Baker, D.B. Total synthesis of the antitumor antibiotic (±)-streptonigrin: First- and second-generation routes for de novo pyridine formation using ring-closing metathesis. *J. Org. Chem.* **2013**, *78*, 12338–12350. [CrossRef] [PubMed]
21. Kadela-Tomanek, M.; Bębenek, E.; Chrobak, E.; Boryczka, S. 5,8-Quinolinedione scaffold as a promising moiety of bioactive agents. *Molecules* **2019**, *24*, 4115. [CrossRef] [PubMed]
22. Kadela-Tomanek, M.; Jastrzębska, M.; Chrobak, E.; Bębenek, E.; Latocha, M. Hybrids of 1,4-quinone with quinoline derivatives: Synthesis, biological activity, and molecular docking with DT-Diaphorase (NQO1). *Molecules* **2022**, *27*, 6206. [CrossRef] [PubMed]
23. Kadela-Tomanek, M.; Jastrzębska, M.; Marciniec, K.; Chrobak, E.; Bębenek, E.; Latocha, M.; Kuśmierz, D.; Boryczka, S. Design, synthesis and biological activity of 1,4-quinone moiety attached to betulin derivatives as potent DT-diaphorase substrate. *Bioorg. Chem.* **2021**, *106*, 104478. [CrossRef]
24. Mulchin, B.; Newton, C.G.; Baty, J.W.; Grasso, C.H.; Martin, W.J.; Walton, M.C.; Dangerfield, E.M.; Plunkett, C.H.; Berridge, M.V.; Harper, J.L.; et al. The anti-cancer, anti-inflammatory and tuberculostatic activities of a series of 6,7-substituted-5,8-quinolinequinones. *Bioorg. Med. Chem.* **2010**, *19*, 3238–3251. [CrossRef]
25. Ling, Y.; Yang, Q.; Teng, Y.; Chen, S.; Gao, W.; Guo, J.; Hsu, P.; Liu, Y.; Morris-Natschke, S.; Hung, C.; et al. Development of novel amino-quinoline-5,8-dione derivatives as NAD(P)H:quinone oxidoreductase 1 (NQO1) inhibitors with potent antiproliferative activities. *Eur. J. Med. Chem.* **2018**, *154*, 199–209. [CrossRef] [PubMed]
26. Ryu, C.; Oh, S.; Choi, S.; Kang, D. Synthesis of antifungal evaluation of 2H-[1,2,3]Triazolo [4,5-g]isoquinoline-4,9-diones. *Chem. Pharm. Bull.* **2014**, *62*, 1119–1124. [CrossRef]
27. Yoo, K.; Yoon, E.; Park, Y.; Park, S.; Lee, C.; Lee, W.; Chi, D.; Kim, D. Synthesis and SAR of aziridinylquinoline-5,8-diones as agents against malignant tumor cells. *Bull. Korean Chem. Soc.* **2001**, *22*, 1067–1068.
28. Kadela-Tomanek, M.; Pawełczak, B.; Jastrzębska, M.; Bębenek, E.; Chrobak, E.; Latocha, M.; Kusz, J.; Książek, M.; Boryczka, S. Structural, vibrational and quantum chemical investigations for 6,7-dichloro-2-methyl-5,8-quinolinedione. Cytotoxic and molecular docking studies. *J. Mol. Struct.* **2018**, *1168*, 73–83. [CrossRef]
29. Jianbo, H.; Tingting, Z.; Yongjing, C.; Yuanyuan, Z.; Weiqing, Y.; Menglin, M. Study on relationship between fluorescence properties and structure of substituted 8-hydroxyquinoline zinc complexes. *J. Fluoresc.* **2018**, *28*, 1121–1126. [CrossRef]
30. Frisch, M.J.; Trucks, G.W.; Schlegel, H.B.; Scuseria, G.E.; Robb, M.A.; Cheeseman, J.R.; Scalmani, G.; Barone, V.; Mennucci, B.; Petersson, G.A.; et al. *Gaussian 16*; Revision A. 03. 2016; Gaussian Inc.: Wallingford, CT, USA, 2016.
31. Wolinski, K.; Hinton, J.; Pulay, P. Efficient implementation of the gauge-independent atomic orbital method for NMR chemical shift calculations. *J. Am. Chem. Soc.* **1990**, *112*, 8251–8260. [CrossRef]
32. Foresman, J.; Frisch, E. *Exploring Chemistry with Electronic Structure Methods: A Guide to Using Gaussian*; Gaussian: Pittsburg, PA, USA, 1996.
33. Politzer, P.; Laurence, P.; Jayasuriya, K. Molecular electrostatic potentials: An effective tool for the elucidation of biochemical phenomena. *Environ. Health Perspect.* **1985**, *61*, 191–202. [CrossRef]
34. Dennington, R.; Keith, T.; Millam, J. *GaussView, Version 5*; Semichem Inc.: Shawnee, KS, USA, 2009.
35. pkCSM. Available online: http://biosig.unimelb.edu.au/pkcsm/prediction# (accessed on 10 January 2023).
36. Pires, D.; Blundell, T.; Ascher, D. pkCSM: Predicting small-molecule pharmacokinetic and toxicity properties using graph-based signatures. *J. Med. Chem.* **2015**, *58*, 4066–4072. [CrossRef] [PubMed]

37. Li, X.; Bian, J.; Wang, N.; Qian, X.; Gu, J.; Mu, T.; Fan, J.; Yang, X.; Li, S.; Yang, T.; et al. Novel naphtho [2,1-d]oxazole-4,5-diones as NQO1 substrates with improved aqueous solubility: Design, synthesis, and in vivo antitumor evaluation. *Bioorg. Med. Chem.* **2016**, *24*, 1006–1013. [CrossRef] [PubMed]
38. Bian, J.; Deng, B.; Xu, L.; Xu, X.; Wang, N.; Hu, T.; Yao, Z.; Du, J.; Yang, L.; Lei, Y.; et al. 2-Substituted 3-methylnaphtho [1,2-b]furan-4,5-diones as novel L-shaped ortho-quinone substrates for NAD(P)H:quinone oxidoreductase (NQO1). *Eur. J. Med. Chem.* **2014**, *82*, 56–67. [CrossRef] [PubMed]
39. Asher, G.; Dym, O.; Tsvetkov, P.; Adler, J.; Shaul, Y. The crystal structure of NAD(P)H Quinone Oxidoreductase 1 in complex with its potent inhibitor dicoumarol. *Biochemistry* **2006**, *45*, 6372–6378. [CrossRef]
40. Trott, O.; Olson, A. AutoDock Vina: Improving the speed and accuracy of docking with a new scoring function, efficient optimization, and multithreading. *J. Comput. Chem.* **2010**, *31*, 455–461. [CrossRef]
41. Dessault Systemes BIOVIA. Available online: https://www.3dsbiovia.com/products/collaborative-science/biovia-discovery-studio/ (accessed on 12 December 2022).
42. Hehre, W.; Ditchfield, R.; Pople, J. Self—Consistent molecular orbital methods. XII. Further extensions of Gaussian-type basis sets for use in molecular orbital studies of organic molecules. *J. Chem. Phys.* **1972**, *56*, 2257–2261. [CrossRef]
43. Cheeseman, J.; Trucks, G.; Keith, T.; Frisch, M. A comparison of models for calculating nuclear magnetic resonance shielding tensors. *J. Chem. Phys.* **1994**, *104*, 5497–5509. [CrossRef]
44. Pérez, P.; Domingo, L.R.; Aurell, M.J.; Contreras, R. Quantitative characterization of the global electrophilicity pattern of some reagents involved in 1,3-dipolar cycloaddition reactions. *Tetrahedron* **2003**, *59*, 3117–3125. [CrossRef]
45. Domingo, L.R.; Ríos-Gutiérrez, M.; Pérez, P. Applications of the conceptual density functional theory indices to organic chemistry reactivity. *Molecules* **2016**, *21*, 748. [CrossRef]
46. Ali, B.; Khalid, M.; Asim, S.; Khan, M.U.; Iqbal, Z.; Hussain, A.; Hussain, R.; Ahmed, S.; Ali, A.; Hussain, A.; et al. Key electronic, linear and nonlinear optical properties of designed disubstituted quinoline with carbazole compounds. *Molecules* **2021**, *26*, 2760. [CrossRef]
47. Zhou, Z.; Liu, Y.; Ren, Q.; Yu, D.; Lu, H. Synthesis, crystal structure and DFT study of a novel compound N-(4-(2,4-dimorpholinopyrido [2,3-d]pyrimidin-6-yl)phenyl)pyrrolidine-1-carboxamide. *J. Mol. Struct.* **2021**, *1235*, 130261. [CrossRef]
48. Marya, Y.S.; Mary, J.; Krátký, M.; Vinsov, J.; Baraldi, C.; Gamberini, M. DFT, molecular docking and SERS (concentration and solvent dependant) investigations of a methylisoxazole derivative with potential antimicrobial activity. *J. Mol. Struct.* **2021**, *1232*, 130034. [CrossRef]
49. Chandrasekaran, K.; Kumar, R. Structural, spectral, thermodynamical, NLO, HOMO, LUMO and NBO analysis of fluconazole. *Spectrochim. Acta A* **2015**, *150*, 974–991. [CrossRef] [PubMed]
50. Jakhar, R.; Dangi, M.; Khichi, A.; Chhillar, A.K. Relevance of molecular docking studies in drug designing. *Curr. Bioinf.* **2019**, *15*, 270–278. [CrossRef]
51. Al-Attraqchi, O.H.A.; Venugopala, K.N. 2D- and 3D-QSAR modeling of imidazole-based glutaminyl cyclase inhibitors. *Curr. Comput. Aided Drug Des.* **2020**, *16*, 682–697. [CrossRef] [PubMed]
52. Delaney, J.S. ESOL: Estimating aqueous solubility directly from molecular structure. *J. Chem. Inf. Model.* **2004**, *44*, 1000–1005. [CrossRef] [PubMed]